Macromolecules

Article

pubs.acs.org/Macromolecules

Thermo-Induced Self-Assembly of Responsive Poly(DMAEMA-*b*-DEGMA) Block Copolymers into Multi- and Unilamellar Vesicles

Christian Pietsch,[†,‡,§] Ulrich Mansfeld,[†,‡,§] Carlos Guerrero-Sanchez,[∥] Stephanie Hoeppener,[†,‡,§] Antje Vollrath,[†,‡] Michael Wagner,[†,‡] Richard Hoogenboom,[⊥] Simon Saubern,[∥] San H. Thang,[∥] C. Remzi Becer,[#] John Chiefari,[∥] and Ulrich S. Schubert*[,†,‡,§]

[†] Laboratory of Organic and Macromolecular Chemistry (IOMC) Friedrich-Schiller-University Jena, Humboldtstrasse 10, 07743 Jena, Germany

[‡] Jena Center for Soft Matter (JCSM), Humboldtstrasse 10, 07743 Jena, Germany

[§] Dutch Polymer Institute (DPI), John F. Kennedylaan 2, 5612 AB Eindhoven, The Netherlands

[∥] CSIRO, Materials Science and Engineering, Bag 10, Clayton South, 3169 Victoria, Australia

[⊥] Supramolecular Chemistry Group, Department of Organic Chemistry, Ghent University, Krijgslaan 281 S4, 9000 Ghent, Belgium

[#] Department of Chemistry, University of Warwick, CV4 7AL Coventry, United Kingdom

Supporting Information

ABSTRACT: A series of thermoresponsive diblock copolymers of poly[2-(dimethylamino)ethyl methacrylate-*block*-di(ethyleneglycol) methyl ether methacrylate], poly(DMAEMA-*b*-DEGMA), were synthesized by reversible addition−fragmentation chain transfer (RAFT) polymerizations. The series consist of diblock and quasi diblock copolymers. Sequential monomer addition was used for the quasi diblock copolymer synthesis and the macro-chain transfer approach was utilized for the block copolymer synthesis. The focus of this contribution is the controlled variation of the ratios of DMAEMA to DEGMA in the copolymer composition, resulting in a systematic polymer library. One of the investigated block copolymer systems showed double lower critical solution temperature (LCST) behavior in water and was further investigated. The phase transitions of this block copolymer were studied in aqueous solutions by turbidimetry, dynamic light scattering (DLS), variable temperature proton nuclear magnetic resonance (^{1}H NMR) spectroscopy, zeta potential, and cryo transmission electron microscopy (cryo-TEM). The block copolymer undergoes a two-step thermo-induced self-assembly, which results in the formation of multilamellar vesicles after the first LCST temperature and to unilamellar vesicles above the second LCST transition. An interplay of ionic interactions as well as the change of the corresponding volume fraction during the LCST transitions were identified as the driving force for the double responsive behavior.

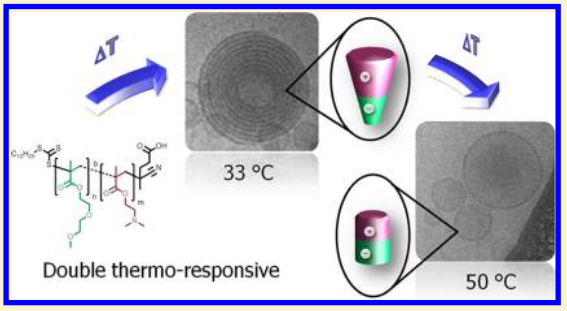

INTRODUCTION

Stimuli-responsive polymers, which undergo phase transitions in response to an external stimulus, have gained the interest of many researchers in the past decade.[1−5] Such "smart" materials can act with a property change in response to changes in temperature, pH value, electric potential, light, or magnetic field.[6−10] The area of stimuli-responsive polymers represents nowadays a strongly growing field in polymer research, in particular the investigation regarding lower critical solution temperature behavior has attracted significant interest. Particular attention in this context has been paid to the thermosensitive self-organization of amphiphilic block copolymers, especially on the formation of micelles or vesicular structures in aqueous solution. Numerous reports on the micellization of diblock copolymers containing thermosensitive block segments are described.[4,6,7,11−13] The formed vesicles or polymersomes are usually spherical shell structures with a hydrophobic core-layer and a hydrophilic internal and external corona made from amphiphilic block copolymers.[14−16] Polymer vesicles, which respond to external stimuli such as a change in temperature or the pH value, represent attractive candidates for applications in encapsulation or drug delivery systems.[3,17,18]

LCST polymers are soluble below a certain temperature because of the formation of hydrogen bonds between water molecules of the hydration shell and the polymer chains. By passing the cloud point temperature (T_{CP}), the polymer starts to precipitate due to the breaking of hydrogen bonds and due to hydrophobic polymer−polymer interactions because the

Received: September 7, 2012
Revised: November 2, 2012
Published: November 19, 2012

   dx.doi.org/10.1021/ma301867h | *Macromolecules* 2012, 45, 9292−9302

Table 1. Overview of the Selected Reaction Conditions Used for the Polymerizations of DMAEMA and DEGMA Using an Automated Parallel Synthesizer

sample	structure	ratio 1st polym DMAEMA/CTA[a]	ratio 2nd polym DEGMA/macroCTA[a]	concn [mol/L]	polym time [h]
H1	homo	90:1		3.0	10.0
B1	quasi		10:1	2.0	6.0
H2	homo	80:1		3.0	10.0
B2	quasi		20:1	2.0	6.0
H5	homo	45:1		3.0	10.0
B5	quasi		55:1	2.0	6.0

[a]Molar ratios of the reaction solution.

entropy term becomes dominant in the Gibbs equation. Besides the gold standard poly(*N*-isopropylacrylamide) (poly(NIPAM)) with a LCST of 32 °C,[1] a number of poly(ethyleneglycol) functionalized (meth)acrylates have been reported to exhibit LCST behavior.[19−21] In particular, different oligo(ethylene glycol) methyl ether methacrylate (OEGMA)-based polymers received significant attention as temperature sensitive materials. The large interest is fueled by the easy preparation of well-defined OEGMA-based copolymers by reversible deactivation radical polymerization (RDRP) techniques such as reversible addition−fragmentation chain transfer (RAFT) polymerizations.[22−24] By variation of the side chain length, the T_{CP} of these copolymers can be tuned, which makes them very attractive systems.[19,25,26] The homopolymer of di(ethylene glycol) methyl ether methacrylate (DEGMA) (two repeating units of ethylene glycol) has a T_{CP} around 27 °C, which can be increased by copolymerizing with a more hydrophilic monomer.[19,20,26,27] 2-(Dimethylamino)ethyl methacrylate (DMAEMA) has been used as such a comonomer, resulting in a pH- and temperature-responsive copolymer.[28] Poly(DMAEMA) is used in various applications, e.g., in gene delivery systems of transfection agents.[29−31] Various T_{CP}'s of poly(DMAEMA) have been reported in literature ranging from 20 to 80 °C, which is an indication that the LCST strongly depends on the used molar masses.[28,32−38] Furthermore, the T_{CP} strongly depends on variations in the pH value due to partial (de)protonation of the basic nitrogen atoms of DMAEMA.[28,35−39]

Block copolymers can be responsive to two different stimuli at the same time, such as temperature and the pH value, as demonstrated for block copolymers of (poly(NIPAM-*b*-AA))[40] and poly(DMAEMA-*b*-MMA).[41] Furthermore, different copolymer brushes of DMAEMA with DEGMA and *tert*-butyl methacrylate (*t*BMA), investigated by Matyjaszewski et al., showed dual responsive properties.[38] The pH and temperature responsive properties were also investigated for different poly(DMAEMA-*co*-DEGMA) hydrogels.[37] Poly(DMAEMA-*b*-DEGMA) block copolymers were recently used to control the self-assembly of virus particles.[42]

The thermoresponsive self-organization of amphiphilic block copolymers in aqueous solution has been described in the literature for several systems.[6,7,11−13,43−47] For example, the self-assembly of double thermoresponsive block copolymers of poly(*N*-*n*-propylacrylamide-*b*-*N*-ethylacrylamide) was reported.[48] Furthermore, the thermo-induced micellization transition of the block copolymer solution of poly(tri(ethylene glycol) methyl ether acrylate)-*b*-poly(4-vinylbenzyl methoxytris(oxyethylene) ether) was described.[49] The formation of double hydrophilic diblock copolymers to vesicle and micelle structures have been studied in detail by Lecommandoux and co-workers using poly((dimethylamino)ethyl methacrylate-*b*-glutamic acid).[50] However, the thermo-induced self-assembly of poly(DMAEMA-*b*-DEGMA) is, to the best of our knowledge, not yet reported.

In this contribution, a series of thermoresponsive diblock copolymers of poly(DMAEMA-*b*-DEGMA) was synthesized by RAFT polymerization ranging from pure block to gradient block copolymer (quasi diblock) structures. The macro-chain transfer approach was used for the preparation of these block copolymers. The ratios of DMAEMA to DEGMA were systematically varied, while the degree of polymerization was kept constant. The self-assembly behavior as well as the LCST of the responsive polymers were measured by turbidimetry. Within this series of block copolymers, a double-responsive behavior was observed for one particular composition and the self-assembly characteristic was further investigated by dynamic light scattering, temperature-dependent ^{1}H NMR spectroscopy, zeta potential analysis, and cryogenic transmission electron microscopy. The formation of spherical structures, like multilamellar and unilamellar vesicles at elevated temperatures, was observed and a model for the formation of these structures was developed.

EXPERIMENTAL SECTION

Materials. Di(ethylene glycol) methyl ether methacrylate (DEGMA) and 2-(dimethylamino)ethyl methacrylate (DMAEMA) were purchased from Sigma-Aldrich and purified by stirring in the presence of inhibitor-remover for hydroquinone or hydroquinone monomethyl ether (Aldrich) for 30 min prior to use. The initiator, 1,1′-azobis(cyclohexane carbonitrile) (VAZO-88), was obtained from DuPont. 4-Cyano-4-[(dodecylsulfanylthiocarbonyl)sulfanyl]pentanoic acid (DTTCP) chain transfer agent (CTA) was prepared according to a literature procedure.[23,51] All analytical grade solvents were purchased from Sigma-Aldrich or Merck KGaA.

Polymerization in an Automated Parallel Synthesizer. The quasi block copolymerizations were performed in a Chemspeed Accelerator SLT automated synthesizer using the sequential monomer addition and following similar experimental procedures as reported elsewhere.[52−54] In a typical polymerization experiment, 864 mg of DMAEMA monomer (5.5×10^{-3} mol), 0.73 mg of VAZO-88 initiator (3.0×10^{-6} mol), 24.1 mg of DTTCP (used as a CTA) RAFT agent (6.00×10^{-5} mol), and *N*,*N*-dimethylformamide (DMF) were mixed together in a 13 mL glass reactor of an automated parallel synthesizer as follows: DMAEMA monomer, DMF solvent reservoir, and individual stock solutions of VAZO-88 (initiator) and DTTCP (CTA) dissolved in DMF were degassed by sparging nitrogen for at least 15 min prior to use. All these reagents were added and combined into one of the reactors of the parallel synthesizer using its automated liquid handling system in order to reach the aforementioned amounts and a monomer concentration of 3.0 M; the ratio of RAFT agent to initiator was 1:0.05. Trioxane dissolved in the DMAEMA monomer was utilized, at a concentration of 5 mg mL^{-1} of total reaction mixture, as internal standard to determine the monomer conversion by ^{1}H

dx.doi.org/10.1021/ma301867h | Macromolecules 2012, 45, 9292−9302

NMR measurements in deuterated chloroform ($CDCl_3$). Once in the reactor, the reaction mixture was subjected to three freeze−pump−thaw cycles between −70 and −10 °C (5 mbar vacuum for 2 min each cycle) in the parallel synthesizer.[53] Thereafter, the reaction mixtures were heated up to 90 °C and vortexed at 600 rpm for 10 h; the coldfinger reflux condensers were set to 7 °C during the reaction. After the polymerization, samples of 75 μL were withdrawn with the liquid handling system of the apparatus and transferred into NMR tubes and size exclusion chromatography (SEC) vials, which were filled with their corresponding solvent for analysis. The first polymerization step proceeded up to a certain conversion, which resulted in a poly(DMAEMA) macro-chain transfer agents (macro-CTAs). Thereafter, the polymers were chain extended with DEGMA using similar conditions as described above. The DEGMA concentration was kept at 2.0 mol L^{-1} for each polymerization experiment. Table 1 summarizes the utilized reaction conditions and [M]/[CTA] ratios. After completion of the polymerization, dichloromethane (CH_2Cl_2) was added to the final mixtures and the polymers were then manually precipitated into *n*-hexane (with adding CH_2Cl_2, DMF is soluble in *n*-hexane). Afterward, the copolymers were dried in a vacuum oven at 40 °C.

Polymerization via Classical Conditions. Block copolymers were also synthesized using the macro-CTA approach with a precipitation step in between to obtain pure block segments. The desired amounts of the monomer (e.g., 2.36 g, 15.0 mmol of DMAEMA) were transferred into Schlenk type reactors and were diluted with DMF. Thereafter, the calculated volumes of stock solutions of CTA (DTTCP, 0.15 mmol, 60.55 mg) as well as the initiator (VAZO-88, 0.008 mmol, 1.83 mg) were added. The ratio between [CTA] and [VAZO-88] was 1:0.05. The prepared solutions were degassed using four freeze−pump−thaw cycles. Subsequently, the reaction was performed in an oil bath at 90 °C for 10 h. After the polymerization, CH_2Cl_2 was added to the final mixtures and the polymers were then manually precipitated into *n*-hexane (with adding CH_2Cl_2, DMF is soluble in *n*-hexane). Afterward, the polymers were dried in a vacuum oven at 40 °C. The final poly(DMAEMA)s were used as a macro-CTA and chain extended with DEGMA using similar conditions as described above. The utilized reaction conditions and [M]/[CTA] ratios are summarize in Table 2. All monomer conversions were measured by ^{1}H NMR spectroscopy using trioxane as internal standard. The molar masses of the obtained polymers were measured by SEC.

Instrumentation. Size-exclusion chromatography (SEC) was performed on a system comprising a Waters 590 HPLC pump and a Waters 410 refractive index detector equipped with three Waters Styragel columns (HT2, HT3, HT4, each 300 mm × 7.8 mm, providing an effective molar mass range of 100−600000 g mol^{-1}). The eluent was DMF (containing 0.45% w/v LiBr) at 80 °C with a flow rate of 1 mL min^{-1}. Number (M_n) and weight-average (M_w) molar masses were evaluated using Waters Millennium software. A polynomial was used to fit the log *M* vs time calibration curve, which was linear across the molar mass ranges. The SEC columns were calibrated with low polydispersity polystyrene standards (Polymer Laboratories) ranging from M_n 3100 to 650000 g mol^{-1}. Further SEC experiments were performed on a Shimadzu system equipped with a SCL-10A system controller, a LC-10AD pump, a RID-10A refractive index detector, and a PSS SDV linear S, 5 μm column (8 mm × 300 mm) with chloroform/triethylamine/2-propanol (94:4:2) as eluent, and the column oven was set to 40 °C. A calibration with low polydispersity polystyrene standards (ranging M_n from 376 to 128000 g mol^{-1}) was used. In addition, further SEC experiments were carried out using an Agilent1200 series system, a G1310A pump, a G1362A refractive index detector, and both a PSS Gram30 and a PSS Gram1000 column in series, whereby *N*,*N*-dimethylacetamide (DMAc) with 5 mmol lithium chloride was used as an eluent at 1 mL min^{-1} flow rate, and the column oven was set to 40 °C. The system was calibrated with polystyrene (M_n from 374 g mol^{-1} to 1040000 g mol^{-1}) standards. Proton nuclear magnetic resonance (^{1}H NMR) spectra were recorded on a Bruker AC 300 (300 MHz) and 400 (400 MHz) spectrometer at 298 K. The chemical shifts are reported in parts per million (ppm, δ scale) relative to the signals from the NMR solvents. The temperature variable ^{1}H NMR spectroscopy was recorded on a Bruker AC 400 (400 MHz) spectrometer in deuterium oxide (D_2O) at a polymer concentration of 5.0 mg mL^{-1}. At each temperature step (5 °C) from 25 to 65 °C, the polymer solution was equilibrated for 3 min. Conversions were calculated from ^{1}H NMR spectra using 1,3,5-trioxane as an internal standard. The cloud point measurements for the identification of the LCST behavior were performed by heating the polymer (1.0, 2.5, 5.0, and 10.0 mg mL^{-1}, respectively) in deionized water from 0 to 105 °C with a heating rate of 1.0 °C min^{-1} followed by cooling to 0 °C at a cooling rate of 1.0 °C min^{-1} after keeping it 10 min at 105 °C. This cycle was repeated three times. During these controlled cycles, the transmission through the solutions was monitored in a Crystal16 from Avantium Technologies. The cloud points are reported as the 50% transmittance temperature in the second heating run.

High-throughput dynamic light scattering (HT-DLS) measurements were performed on the DynaPro Plate Reader Plus (Wyatt Technology Corporation, Santa Barbara, CA) equipped with a 60 mV linearly polarized gallium arsenide (GaAs) laser of λ = 832.5 nm and operating at an angle of 156°. The samples were heated from 25 to 65 °C in a 96-well plate using 10 °C heating steps, and after 5 min equilibration time, each well was measured collecting five acquisitions. The data were analyzed with the Dynamics software version 6.20 by the method of cumulants.[55] The percent of polydispersity is given by $\%Pd = 100(\mu_2)/\mu_1^2$, where μ_1 and μ_2 are the first- and the second-order cumulant, respectively. The level of homogeneity is considered high when the percent polydispersity is less than 15%. If the level of homogeneity is low (percent polydispersity larger than 30%), the particle population can be considered as being polydisperse. DLS measurements were also carried out on a Zetasizer Nano ZS (Malvern Instruments, Malvern, UK) operating with a laser beam at 633 nm and a scattering angle of 173°. The sample was heated in a quartz cuvette from 25 up to 65 °C in 1 °C steps. At each temperature step, the sample was equilibrated for 120 s and then measured three times including three runs for 30 s. The intensity and the volume distribution of the particle size were calculated applying the NNLS mode.

Electrophoretic light scattering was used to measure the electrokinetic potential, also known as zeta potential. The measurements were performed using a Zetasizer Nano ZS (Malvern Instruments) by applying laser Doppler velocimetry. For each measurement, 20 runs were carried out using the slow-field reversal and fast-field reversal mode at 150 V. Each experiment was performed in triplicate from 25 to 65 °C in 5 °C steps. The zeta potential (ζ) was calculated from the electrophoretic mobility (μ) according to the Henry equation. The Henry coefficient *f*(ka) was calculated according to Oshima.[56]

Table 2. Overview of the Selected Reaction Conditions Used for the Polymerizations of DMAEMA and DEGMA via the Schlenk Technique

sample	structure	ratio feed 1st polym monomer/CTA[a]	ratio feed 2nd polym monomer/macroCTA[a]	concn [mol/L]	polym time [h]
H3	homo	(DMAEMA) 100:1		2.0	10.0
B3	block		(DEGMA) 100:1	1.0	7.5
H4	homo	(DMAEMA) 100:1		3.0	8.0
B4	block		(DEGMA) 100:1	1.0	6.0
H6	homo	(DEGMA) 100:1		2.0	8.0
B6	block		(DMAEMA) 50:1	1.0	6.0

[a]Molar ratios of the reaction solution.

Scheme 1. Schematic Representation of the Poly(DMAEMA-*b*-DEGMA) Formation Using RAFT Polymerization with the CTA DTTCP and the Radical Initiator VAZO-88

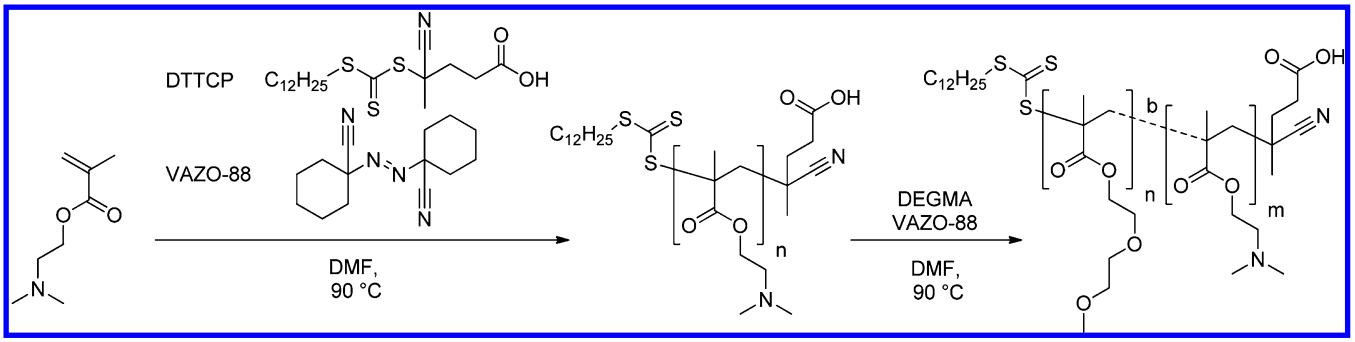

Table 3. Composition of the Block Copolymers of Poly(DMAEMA-*b*-DEGMA) from SEC and ^{1}H NMR Spectroscopy with Increasing Ratio of DEGMA Starting from DMAEMA Homopolymer

	SEC (DMF)[b]		SEC (DMAc)[c]		SEC ($CHCl_3$)[d]				
sample[a]	M_n [g/mol]	PDI	M_n [g/mol]	PDI	M_n [g/mol]	PDI	conv.[e] [%]	$M_{n,theo}$[f] [g/mol]	ratio [%] ^{1}H NMR[g] DMAEMA/DEGMA
H1 (h)	18600	1.16					81 (M1)	10200	100:0
H2 (h)	15200	1.17					62 (M1)	6200	100:0
H3 (h)	17600	1.22					80 (M1)	13000	100:0
H4 (h)	15200	1.21	13500	1.43	28700	1.22	83 (M1)	13300	100:0
H5 (h)	8800	1.16					75 (M1)	5400	100:0
B1 (q)	20800	1.29	24700	1.44	29700	1.36	39 (M2)	12600	94:6
B2 (q)	21800	1.25	24100	1.41	30200	1.34	70 (M2)	10900	87:13
B3 (b)	26900	1.27	27400	1.52	*h*	*h*	65 (M2)	25400	66:34
B4 (b)	35100	1.54	36600	1.48	*h*	*h*	53 (M2)	23300	64:36
B5 (q)	39700	1.35	24000	1.70	*h*	*h*	85 (M2)	15300	51:49
B6 (b)	26600	1.32	27100	1.33	33500	1.24	40 (M1)	20800	20:80
H6 (h)	23600	1.23	23700	1.29	27800	1.20	76 (M2)	14500	0:100

[a]Copolymer structure: h = homopolymer, q = quasi diblock copolymer, b = diblock copolymer. [b]Calculated from SEC (DMF) using PS calibration. [c]Calculated from SEC (DMAc) using PS calibration. [d]Calculated from SEC ($CHCl_3$/triethylamine/2-propanol = 94/4/2) using PS calibration. [e]Calculated from vinyl integrals of ^{1}H NMR spectra using trioxane as internal standard, M1 = DMAEMA and M2 = DEGMA. [f]Calculated according to formula ($M_{n,t\ heo}$ = ([M]/[CTA] × conv × $M_{monomer}$) + M_{CTA}), besides for block copolymers where M_{CTA} is $M_{macroCTA}$. [g]Calculated from integrated areas of DMAEMA signals ($(CH_3)_2N-$) and the DEGMA (CH_2-O-) side-group signals. [h]Block copolymer reached the exclusion limit of the SEC.

Cryogenic transmission electron microscopy (cryo-TEM) measurements were performed on a Philips CM120 operating at an acceleration voltage of 120 kV. Images were recorded with a bottom mounted 1 k × 1 k CCD camera. The samples for TEM investigations were prepared and stored at room temperature prior to the investigation (5 mg mL^{-1}). For the temperature-dependent investigation, the samples were preheated under frequent agitation for at least 30 min in a water bath at 35 and 50 °C, respectively. A drop of the polymer solution (5 μL) was rapidly placed with a preheated microliter pipet on a perforated carbon grid (Quantifoil R2/2) within an in-house-built controlled environment vitrification system (CEVS) with a saturated water atmosphere. The temperature within the CEVS was adjusted to 38 and 55 °C to ensure that the sample is investigated above the corresponding cloud point temperatures. Prior to the blotting, the liquid was allowed to equilibrate on the grids for at least 2 min to avoid preparation artifacts. The controlled saturated humidity and defined temperature minimizes temperature alterations of the sample due to evaporation effects. The samples were rapidly blotted and plunged into a cryogen reservoir containing liquid ethane. After preparation, the samples were stored and measured at a temperature below −176 °C to avoid the formation of crystalline ice layers. To avoid further preparation artifacts, similar blotting times were used at different temperatures.

RESULTS AND DISCUSSION

Synthesis of the Poly(DMAEMA-*b*-DEGMA) Library. A library of double thermoresponsive poly(DMAEMA-*b*-DEGMA) diblock copolymers was synthesized using the RAFT polymerization technique in a sequential monomer addition approach. Within this series, the ratios of DMAEMA and DEGMA were varied ranging from 100% DMAEMA to 100% DEGMA with composition changes in 20% steps. Two possibilities of the macro-chain transfer approach were explored, namely with and without a precipitation step after the first polymerization. Using a parallel robot platform, the second DEGMA monomer was added before the full conversion of DMAEMA was reached, resulting in quasi diblock structures. The polymerizations were carried out using 4-cyano-4-[(dodecylsulfanylthiocarbonyl) sulfanyl]pentanoic acid (DTTCP) as CTA and VAZO-88 as radical initiator (see Scheme 1), applying similar conditions as previously described for the MMA polymerization,[57] namely 90 °C with a ratio of DTTCP to VAZO-88 of 20:1.

The quasi diblock copolymers were synthesized in a Chemspeed Accelerator SLT106 automated platform and the diblock copolymers under classical conditions (Schlenk technique) using the same polymerization conditions. The first block segment was polymerized in DMF at a concentration of 3.0 mol L^{-1}, followed by the polymerization of DEGMA with a monomer concentration of 2.0 mol L^{-1}. For **B6**, this order was reversed, meaning that first DEGMA was polymerized and

dx.doi.org/10.1021/ma301867h | *Macromolecules* 2012, 45, 9292−9302

Table 4. Cloud Point Temperatures from Turbidimetry Measurement of the Homo and Block Copolymers

	cloud points by turbidimetry (2nd heating run) in °C[a]							
sample DMAEMA/DEGMA [%]	**H4** 100:0	**B1** 94:6	**B2** 87:13	**B3** 66:34	**B4** 64:36	**B5**[c] 51:49	**B6** 20:80	**H6** 0:100
10 mg mL^{-1}	45.4	43.6	40.7	m[b]	m[b]	32.5:48.0	29.4	25.1
5.0 mg mL^{-1}	46.7	44.5	41.7	m[b]	m[b]	33:~49 32:~48[d]	30.0	25.9
2.5 mg mL^{-1}	49.0	46.0	43.2	m[b]	m[b]	34:~46	30.5	28.0
1.0 mg mL^{-1}	57.4	48.2	45.3	m[b]	m[b]	~41	31.5	36.4

[a]Estimated in deionized water at 50% transmission for the second heating run. [b]No clear phase separation transition. [c]Estimated at the local maximum at the half %value of transmission. [d]Estimated in D_2O.

then the corresponding DMAEMA block. In Table 3, the molar masses and polydispersity indices (PDI) measured by SEC are summarized, demonstrating good control over the first blocks (PDI < 1.23) and relatively good control for most block copolymers (PDI < 1.35, except **B4**). The obtained diblock copolymers were characterized by SEC in DMF, DMAc, and chloroform as eluent, using a refractive index detector (see Supporting Information (SI)). The hydrodynamic volume of poly(DMAEMA) depends strongly on the solvent and, additionally, it is known that interactions with the column material[58] occur due to the basic nitrogen atoms, therefore, different SEC systems were used to characterize the block copolymers. Nevertheless, the obtained values should be handled with care because of both the calibration with polystyrene and the possibility of column interactions.[59]

The monomer conversions of DMAEMA and DEGMA were estimated by ^{1}H NMR spectroscopy. The conversion of DMAEMA was around 70−80% after 10 h of polymerization. Then the polymerization was stopped to retain high RAFT end-group functionality. A clear molar mass shift could be observed for the block copolymers in the SEC analysis. For the final copolymers, the ratio between both block segments were determined by ^{1}H NMR spectroscopy using the integrated areas of DMAEMA signals ($(CH_3)_2N-$ at 2.26 ppm) and the DEGMA (CH_2-O- at 3.54−3.66 ppm) ethylene glycol side-group signals (Figure S6, SI). The observed ratios are in a good agreement with the monomer feed ratio.

Thermoresponsive Properties of Poly(DMAEMA-*b*-DEGMA). Heating solutions of the polymers in deionized water induces a LCST transition, i.e., the solutions become turbid above the characteristic T_{CP}, indicating the collapse of the polymer chains (two-phase system). The T_{CP}'s of the homo- and block copolymers were determined by turbidimetry measurements in deionized water at four different concentrations (1.0, 2.5, 5.0, and 10.0 mg mL^{-1}) and are listed in Table 4. All thermo-induced transitions of the copolymers were found to be fully reversible (SI, Figure S7).

The T_{CP} of the homopolymer poly(DEGMA), **H6**, is 25.9 °C at 5.0 mg mL^{-1}, which correspond well with the literature value of 27 °C.[19,20,27] With increasing amount of DMAEMA, the observed demixing points increase and the highest T_{CP} is observed for the homopolymer of poly(DMAEMA), **H4**, namely 46.7 °C at 5.0 mg mL^{-1} (see also Figure 1). This observed effect is due to the increased hydrophilicity of the "end-group" by the incorporation of the PDMAEMA block. In some cases, namely for **B3** and **B4**, the solutions showed only weak transitions, presumably due to the formation of mainly smaller aggregates. All T_{CP} transitions from the turbidimetry measurement of the block copolymers are plotted in Figure 1 against the molar ratio of PDMAEMA to provide a better

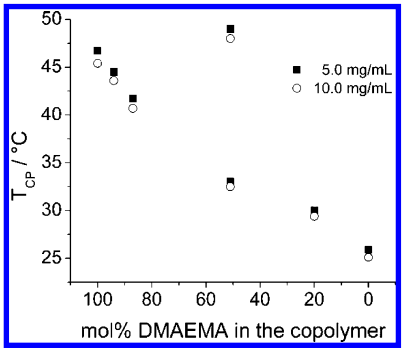

Figure 1. Cloud points (T_{CP}) of the studied block copolymers of poly(DMAEMA-*b*-DEGMA) at 5.0 and 10.0 mg mL^{-1}.

overview. A roughly linear behavior of the T_{CP} transitions with increasing amount of mol% DMAEMA in the block copolymers could be observed. Differences between the pure and the quasi diblock copolymer were not observed in the turbidimetry measurements; apparently the gradient is too small to have an influence. For all samples, a lower T_{CP} is observed with higher concentration due to the statistical influence during the aggregation behavior. Two T_{CP} values were observed for **B5** (see Table 4 and Figure 1), indicating the double thermo-responsive behavior in aqueous solution. The turbidimetry curve of this copolymer shows a weak transition at 33 °C followed by a rearrangement and, therefore, a second transition at 49 °C (see also Figure S8 SI).

Due to its double-responsive behavior, the **B5** block copolymer was selected for detailed structural analysis, as it shows the most interesting thermoresponsive behavior of the tested copolymers.

The LCST transition was further investigated in detail by DLS measurements as function of temperature for **B5**. To efficiently characterize different concentrations of this block copolymer, a high-throughput DLS plate reader setup was used. The demixing values were estimated by this DLS setup in deionized water at four different concentrations (1.0, 2.5, 5.0, and 10.0 mg mL^{-1}) starting from 25 °C and heating up to 65 °C in 10 °C steps. The temperature induced collapse of the quasi diblock copolymer **B5** (~50% of each block segment) resulted in the appearance of two size distributions (Figure 2), one with a diameter of 40 nm and a second of around 300 nm. The size of the agglomerates of **B5** is nearly constant also by further increasing the temperature. In addition, the polymer concentration has no significant influence on the size of the self-assembled structures of the block copolymer. The self-assembled structures might be micelles (ca. 40 nm) and larger vesicular structures (300−400 nm), although no conclusive assignment can be made based on the DLS results alone. To

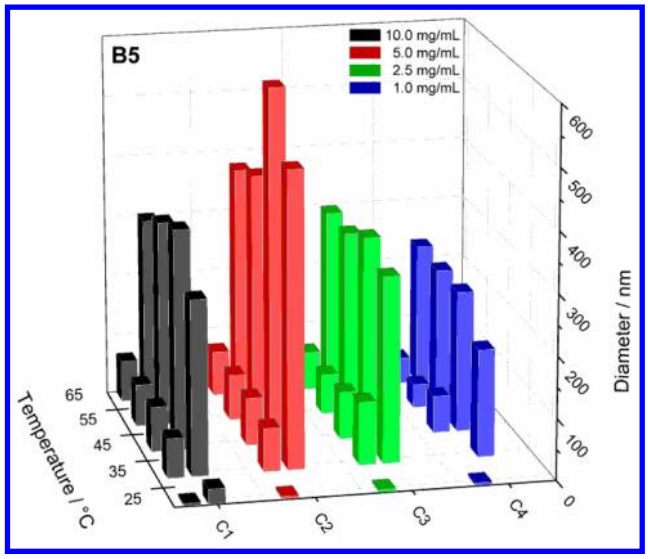

Figure 2. Hydrodynamic diameters of the copolymer coils and globules of **B5** (showing two distribution) at different concentration as function of temperature.

evaluate the aggregation behavior of the chosen copolymer, **B5** was investigated in further detail using a DLS Zetasizer (Malvern).

The experiment was performed in deionized water at a concentration of 1.0 mg mL^{-1}, and the temperature run was set up between 25 and 50 °C, with heating in 1 °C steps to have a closer look at the phase transitions. A repeated temperature run ranging from 25 to 65 °C is plotted in the SI (Figure S10), showing a similar size distribution of the observed self-assembled aggregates. No changes in the size above 50 °C are observed. The distribution of the block copolymer assemblies at temperatures below and above the phase transition is illustrated in Figure 3 (volume distribution; intensity distribution is plotted in the SI, Figure S10). Below the cloud point at 25 °C, the polymer chains are fully soluble and, therefore, a hydrodynamic diameter smaller than 10 nm was obtained, corresponding most probably to individual hydrated polymer chains, taking into account also the molecular dimensions of the block copolymers. An increase in temperature results in an increase in the diameter of the polymer aggregates to ∼100 nm, indicating the temperature-induced aggregation of the polymer chains. The first transition of the polymer solution is observed at a temperature of 31 °C, i.e., when the collapse of the PDEGMA takes place.

The hydrodynamic diameter of these aggregates is around 100 nm as displayed in Figure 3. By further increasing the temperature, a rearrangement is observed, which is reflected in the appearance of a second distribution. Above 36 °C, two distributions are formed with a hydrodynamic diameter of 65 and 240 nm, respectively. The formed structures appear to be thermodynamically stable in solution, as the aggregate size remains constant even at further increased temperatures.

The temperature induced phase transition of the selected block copolymer **B5** was further investigated by temperature dependent ^{1}H NMR spectroscopy to obtain a deeper insight into the aggregation behavior. The phase transition was investigated in D_2O at a concentration of 5.0 mg mL^{-1}. At each temperature step (5 °C), the polymer solution was equilibrated for 3 min (it should be noted here that the time scale of the temperature induced formation of micellar structures and larger aggregates is faster than the typical acquisition times required by the NMR spectrometer). The ^{1}H NMR spectrum of the block copolymer at 25 °C shows the characteristic signals of poly(DMAEMA-*b*-DEGMA); the corresponding temperature series is plotted in Figure 4. In the ^{1}H NMR spectra, the signals at 3.3−3.9 ppm represent the ethylene glycol and $-OCH_3$ groups (EG) of poly(DEGMA)

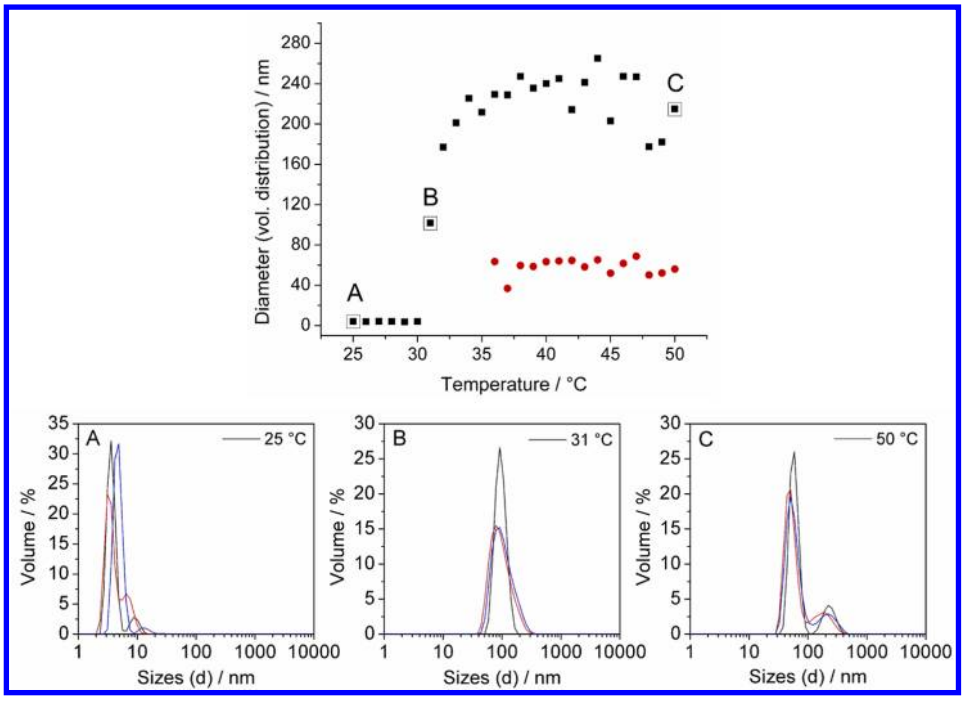

Figure 3. The hydrodynamic diameter (volume distribution, average value of three estimations) of the block copolymer chains and globules of **B5** at 1.0 mg mL^{-1} is plotted as a function of temperature. (A−C) Hydrodynamic size distribution (three measurements) at the respective temperature.

dx.doi.org/10.1021/ma301867h | *Macromolecules* 2012, 45, 9292−9302

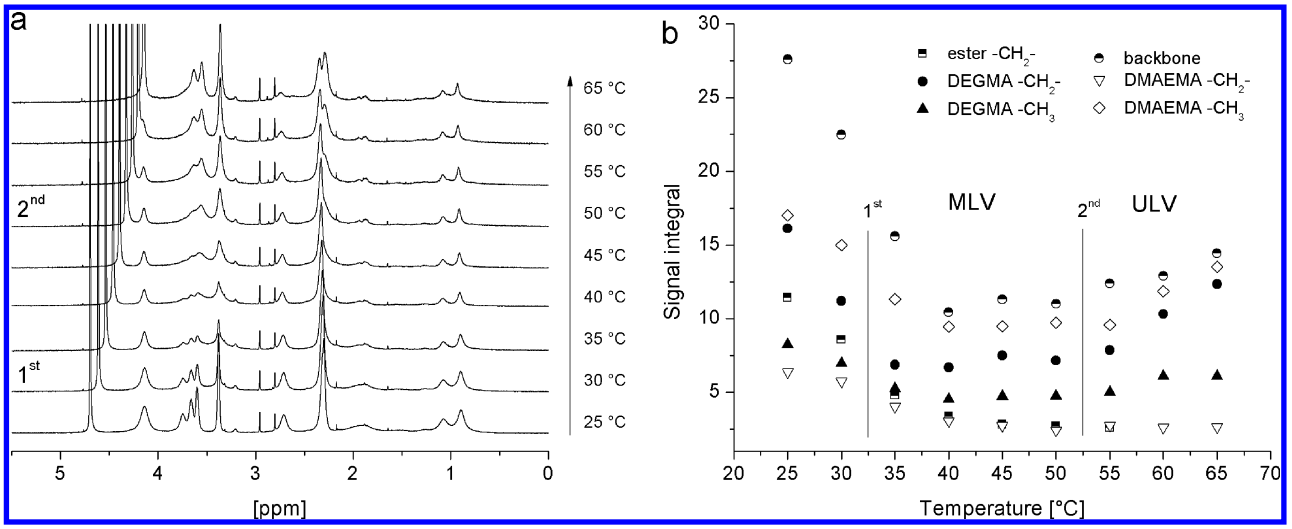

Figure 4. Temperature dependent ^{1}H NMR spectra (a) in D_2O of **B5** (5 mg mL^{-1}) showing the evolution of the $-CH_2-$ and CH_3- signals of poly(DEGMA) block at 3.3 ppm and 3.5−3.9 ppm, and the $-CH_2-$ and CH_3-resonance of the poly(DMAEMA) block segment at 2.7 and 2.3 ppm as well as the polymer backbone in a temperature range from 25 to 65 °C. On the right side (b), the integrals of the block copolymer signals are plotted against the temperature (MLV = multilamellar vesicles and ULV = unilamellar vesicles, see also Figures 5 and 6).

and the signals at 2.3 ppm (CH_3-N-) represent the poly(DMAEMA) block. The position of the small DMF signals, which are left after the precipitation and drying processes, were used as reference signal (adjustment of changes due to the temperature increase, whereby the DMF is unaffected) and all spectra were normalized in intensity to the D_2O signal. It is observable (Figure 4) that the DEGMA signals at 3.5−3.9 ppm decrease significantly, denoting the collapse of the DEGMA block which is induced by the temperature increase from 25 to 40 °C. Also, all other signals (backbone at 0.8−1.5 ppm and DMAEMA at 2.3 and 2.8 ppm) decrease by increasing temperature, leading to broad signals due to the reduced flexibility of the polymer chains (see Figure 4). The PDMAEMA block is still visible at 45 °C (CH_3-N- at 2.2 ppm) as it is supposed that it forms a kind of corona around the hydrophobic PDEGMA aggregates.

Unexpectedly, further increasing the temperature from 50 to 65 °C is accompanied by an increase for some signals corresponding to DMAEMA and to DEGMA (Figure 4b), respectively. These signals are visible for the DMAEMA group (CH_3-N-) at 2.2 ppm, for the EG groups of DEGMA at 3.6 and 3.7 ppm as well as for the $-OCH_3$ group at 3.3 ppm. The shifted signals indicate a different microenvironment of (at least parts of) the DMAEMA and DEGMA groups and are supposed to correlate to the corresponding rearrangement of the block copolymer. This second assembly might be induced by the collapse of the DMAEMA block (at 49 °C vs the homopolymer of poly(DMAEMA) at 47 °C as listed in Table 4 for a concentration of 5.0 mg mL^{-1}), which appears to be at these temperatures more hydrophobic than in the previous configuration (hydrophilic corona), thus resulting in a structural change. The transformation of the PDMAEMA block is indicated by the high-field shift of the DMAEMA signal, which provides a higher electron density at the methyl groups (CH_3-N-) caused by the breaking of the H-bonds.

There might also be a migration of the more polar DEGMA groups (higher amount of oxygen atoms in the structure) to the surface of the collapsed structures to stabilize them in aqueous solution. This migration could lead then to a partial hydration of the DEGMA chains, which causes the reappearance of the corresponding signals in the NMR spectra (Figure 4a at 3.6−3.7 ppm).

Self-Assembly of Poly(DMAEMA-*b*-DEGMA). The double responsive behavior of poly(DMAEMA-*b*-DEGMA) motivated the utilization of cryo-TEM to visualize the associated structures. The sample preparation was performed at different temperatures, and the samples were instantaneously vitrified after an equilibration time of ∼2 min to preserve the aggregate structure at the blotting temperature. The cryo-TEM images of solutions which were vitrified at a blotting temperature of approximately 33 °C are depicted in Figure 5.

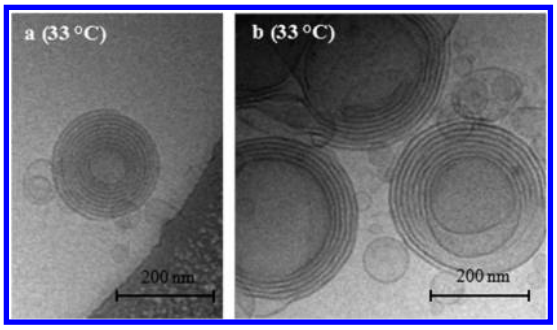

Figure 5. Cryo-TEM images (a,b) of **B5** block copolymer solution at ∼33 °C in H_2O (preheated, 5.0 mg mL^{-1}) showing the formation of multilamellar vesicles and additionally unilamellar vesicles.

At this temperature, which is above the T_{CP} of PDEGMA and below the T_{CP} of PDMAEMA, the presence of large multilamellar vesicles (MLV) with a diameter of approximately 200 nm and unilamellar vesicles (ULV), which are observed to be significantly smaller (40 to 90 nm), is observed. The cryo-TEM micrograph shows that the MLVs have a layered structure with comparable distance between the individual lamellae and represent an onion-like form. In this case, a molecular arrangement of the copolymer can be assumed that resembles the structure depicted in Figure 5 (PDEGMA dark; PDMAEMA light).

The formation of MLV is based on one hand on the hydrophilic−hydrophobic character of the block copolymers

dx.doi.org/10.1021/ma301867h | *Macromolecules* 2012, 45, 9292−9302

and on the other hand on the volume fractions of the individual blocks, respectively. The self-assembly of amphiphiles into well-defined structures, such as vesicles, derives from the hydrophobic attraction at the hydrocarbon−water interface, which induces the molecules to associate, and the hydrophilic part that remain in contact with water.[60] For thermosensitive block copolymers, the individual blocks shows a selective, thermally driven solubility and, therefore, the overall hydrophilic−hydrophobic character can be changed by temperature. At 33 °C, the PDEGMA block is collapsed and therefore hydrophobic, while the PDMAEMA block is hydrophilic and is still in solution due to the fact that the blotting temperature remains below the T_{CP} of PDMAEMA.

The formation of micelles or vesicle structures depends for block copolymers on their ratio between both hydrophobic and hydrophilic segments.[6,7,45,60] Classically, the "critical packing parameter" is used to define the morphology of the resultant self-assembled structure. The ratio of DMAEMA to DEGMA in the block copolymer **B5** is 51% to 49%. With this composition, the formation of micelles or vesicles can be expected.[6,45] In the present case, the block copolymers revealed a tendency for the formation of multilamellar vesicles. The number of shells in these MLVs is up to nine layers for the block copolymer with a significant size distribution of the formed MLVs. The measured size of the different vesicles is between 225 nm (Figure 5a) and 325 nm (Figure 5b), which is in the same size range as obtained by the DLS measurements (approximately 220 nm). The shell thickness of the MLV of PDMAEMA block (Figure 5a) is approximately 5−8 nm. This value is significantly smaller and can be correlated to the polymer chain length (DMAEMA block has DP of ∼45, which equals the length of 11.5 nm when completely stretched) to an interdigitated, very compact arrangement of the PDMAEMA chains.[60] This observation is also supported by the NMR investigations, which show reduced signals of the PDMAEMA block at this temperature. The precipitated PDEGMA core is approximately 6 nm in thickness, which suggests very densely packed chains, which is also supported by the strong dark contrast which is found in the cryo-TEM images.

The polymer was subsequently heated to a temperature above the T_{CP} of DMEAEMA, and the resulting structures were investigated by means of cryo-TEM in the same fashion as described above. In contrast to the sample which was investigated at 33 °C, the formation of preferentially unilamellar, large vesicles is observed. MLVs with a large number of shells are not observed anymore. In Figure 6, the cryo-TEM images of **B5** block copolymer solution acquired at ∼50 °C (a,b) showed the formation of large unilamellar vesicles in aqueous solution.

The thermoresponsive behavior of the selected block copolymer **B5** was further investigated by temperature variable zeta potential (also known as electrokinetic potential) measurements to gain a deeper insight in the polyelectrolyte nature of the block copolymer during the polymer phase transitions (Figure 7). The phase transition was investigated in water at a concentration of 2.5 mg mL^{-1} in the temperature range from 25 to 65 °C during both heating and cooling with temperature steps of 5 °C. The conductivity (red cycles, Figure 7) of the copolymer solution was also measured, indicating a small increase of charge carrier mobility or concentration with increasing temperature, i.e., caused by the increased autodissociation of water. After the cooling cycle, the conductivity of the solution reaches nearly the starting value at 25 °C. The zeta

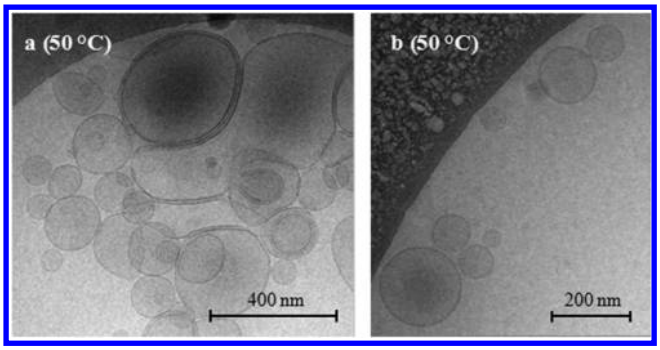

Figure 6. Cryo-TEM image (a,b) of **B5** block copolymer solution at ∼50 °C in H_2O (preheated, 5.0 mg mL^{-1}) showing the formation of large unilamellar vesicles.

potential measurements show that two reversible thermo-induced transitions are present without showing any hysteresis behavior in the graph (Figure 7, black squares). The first transition takes place at around 30 °C and the second transition around 55−60 °C, whereby a strong decrease in the zeta potential is observed. Over the measured temperature range from 25 to 65 °C, a positive potential was measured due to the cationically charged protonated DMAEMA groups. The high value of the zeta potential indicates stable aggregates (usually a potential >25 mV indicates a stable system), which cannot further assemble together due to repulsion forces. In contrast, the pure PDEGMA homopolymer **H6** revealed a negative potential (partially negative charges due to oxygen atoms and carboxylic acid end groups) over the complete temperature range (see SI, Figure S11). On the basis of these results, it can be assumed that the collapse of the PDEGMA block at 30 °C is associated with an enhancement of the negative charges on the surface of the collapsed aggregates (SI, Figure S11), which support the formation of MLVs. The assembly is promoted by electrostatic interactions between the positive charged PDMAEMA block (corona) and the negatively charged collapsed PDEGMA block. This layer-by-layer assembly above the first transition temperature lowers the overall zeta potential of the aggregates. The charge compensation by the layer-by-layer assembly in MLV structures represents an important thermodynamic contribution to the stability of the self-assembled structures. If the temperature is raised above 50 °C, the DMAEMA block starts to collapse. During this collapse, a migration of the DMAEMA chains to the hydrophobic surface of the PDEGMA layer might occur as observed by ^{1}H NMR. This effect changes the electrostatic balance of the MLV structures, i.e., the charge compensation, and ultimately leads to the preferential formation of ULV structures. This change of the charge balance is reflected in the corresponding zeta potential values (Figure 7).

On the basis of these experimental observations, a model for the aggregation of the double responsive transition of the block copolymer structures at different temperatures was developed, which is schematically illustrated in Figure 8. In this configuration, the PDEGMA block (negatively charged) becomes insoluble at the first LCST transition temperature and is collapsed in the lamellar structure. The still-soluble PDMAEMA block (positively charged) stabilizes the individual shells by a layer-by-layer assembly and promotes the preferential formation of multilamellar onion-like vesicles. With further increasing temperature also the solubility of the PDMAEMA decreases. As a result, the volume of the

dx.doi.org/10.1021/ma301867h | *Macromolecules* 2012, 45, 9292−9302

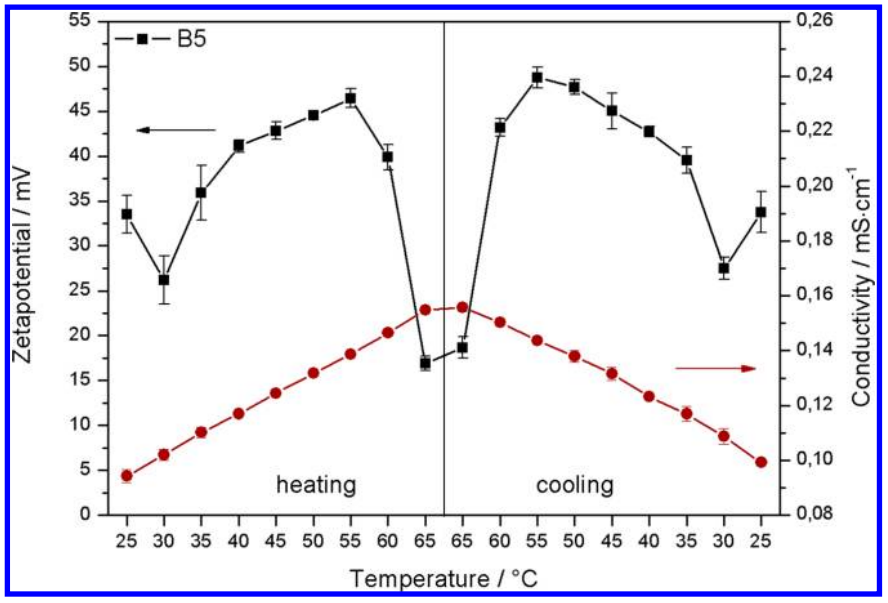

Figure 7. Temperature variable zeta potential measurements (black squares, average value of five estimations) of block copolymer **B5** solution at 2.5 mg mL^{-1} showing two reversible temperature-induced transitions. Also the conductivity (red cycles) of the copolymer solution was measured.

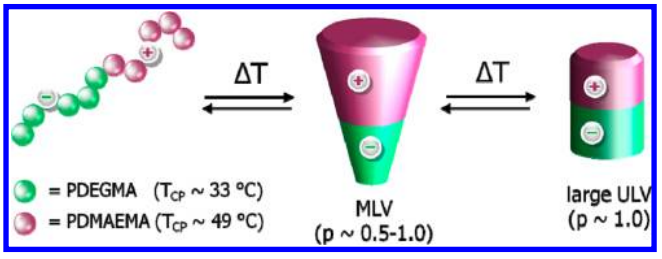

Figure 8. Proposed model for the aggregation of the double responsive transition of the block copolymer. In the figure, represent red cycles DEGMA and green cycles DMAEMA units.

hydrophobic part of the copolymer increases and the interbilayer energy changes. Simultaneously, the decreasing size of the hydrophilic corona block is seen as an additional driving force for the modified aggregation behavior due to altered volume fraction and space requirements.

This effect was, e.g., observed for PS-*b*-PAA aggregates,[61] where shorter corona fractions generally resulted in the formation of larger structures.[62] Additionally, the altered charge balance within the structures favors the formation of larger and unilamellar vesicles.

This structural transitions explain also the ^{1}H NMR observations showing that after the first transition the respective poly(DEGMA) signals disappeared. This could be a direct consequence of the narrow environment, which is formed in the multilamellar vesicle system. As observed from the cryo-TEM images, it can be assumed that above 50 °C a structural transition toward unilamellar vesicles takes place. In this configuration, the packing density of the macromolecules becomes less pronounced, which could be a possible explanation of the reappearance of the poly(DMAEMA) signal in the ^{1}H NMR spectrum.

CONCLUSION

The RAFT polymerization method was used for the preparation of a library of double thermoresponsive diblock copolymers, namely poly(DMAEMA-*b*-DEGMA). A series of poly(DMAEMA-*b*-DEGMA) copolymers have been prepared, with compositions ranging from PDMAEMA to PDEGMA in steps of 20 mol%. The phase transitions of these block copolymers in aqueous solutions were studied in detail by turbidimetry. Higher cloud points of the poly(DMAEMA-*b*-DEGMA) with increasing amount of mol% DMAEMA in the block copolymer were observed. Within this series of block copolymers, a block ratio of 50:50 resulted in a double-responsive LCST behavior. This block copolymer was further investigated to elucidate the self-assembly behavior in detail. Variable temperature ^{1}H NMR spectroscopy, zeta potential, and cryo-TEM investigations revealed the temperature induced formation of multilamellar vesicular structures at elevated temperature which convert into unilamellar vesicles at higher temperatures. On the basis of the measurements, an illustrative model for the reversible temperature-induced self-assembly is given based on the initial formation of multilamellar vesicular (MLV) aggregates that further assemble into unilamellar vesicle (ULV) structures. This transition could be assigned to the changes of the volume ratios as well as to the ionic interplay between the block copolymers at different temperatures. In particular, the ionic contributions of the negatively charged PDEGMA block and the positively charged PDMAEMA block are supposed to support the layer-by-layer assembly at 33 °C, which favors the formation of multilamellar vesicles (MLV). Further increase of the temperature changes again the volume ratio between the blocks as the solubility of the second block occurs, furthermore the second LCST transition is associated with a changed electrostatic balance between the blocks. This results in the preferential transition of MLVs to ULVs. The present study assumes a facile interplay of the volume ratio and the changes of the ionic interactions. However, both contributions cannot be separated by the investigation of only one polymer. In further studies, the formation of self-assembled structures of different block copolymers and at different pH values will be investigated to gain a deeper understanding of the aggregation process.

The design and self-assembly of such thermoresponsive migrating block copolymers will provide new possibilities for delivery vehicles (for therapies), e.g., temperature-controlled

dx.doi.org/10.1021/ma301867h | *Macromolecules* 2012, 45, 9292−9302

release of drugs, and will provide important deeper insights into the LCST transition and the formation of MLVs.

■ ASSOCIATED CONTENT

Supporting Information

SEC curves of poly(DMAEMA-*b*-DEGMA), turbidity curves and zeta potential measurements. This material is available free of charge via the Internet at http://pubs.acs.org.

■ AUTHOR INFORMATION

Corresponding Author

*E-mail: ulrich.schubert@uni-jena.de.

Notes

The authors declare no competing financial interest.

■ ACKNOWLEDGMENTS

We thank W. Günther and G. Sentis for the temperature dependent NMR measurements. Financial support of the Dutch Polymer Institute (DPI, technology area HTE) and the Carl-Zeiss-Foundation (Strukturantrag JCSM) is gratefully acknowledged. C.P. acknowledges also financial support by CSIRO.

■ REFERENCES

(1) Schild, H. G. *Prog. Polym. Sci.* **1992**, *17* (2), 163−249.
(2) Gil, E. S.; Hudson, S. M. *Prog. Polym. Sci.* **2004**, *29* (12), 1173−1222.
(3) Schmaljohann, D. *Adv. Drug Delivery Rev.* **2006**, *58* (15), 1655−1670.
(4) Dimitrov, I.; Trzebicka, B.; Müller, A. H. E.; Dworak, A.; Tsvetanov, C. B. *Prog. Polym. Sci.* **2007**, *32* (11), 1275−1343.
(5) Weber, C.; Hoogenboom, R.; Schubert, U. S. *Prog. Polym. Sci.* **2012**, *37* (5), 686−714.
(6) Du, J.; O'Reilly, R. K. *Soft Matter* **2009**, *5* (19), 3544−3561.
(7) Li, M.-H.; Keller, P. *Soft Matter* **2009**, *5* (5), 927−937.
(8) Hu, J.; Liu, S. *Macromolecules* **2010**, *43* (20), 8315−8330.
(9) Pietsch, C.; Schubert, U. S.; Hoogenboom, R. *Chem. Commun.* **2011**, *47* (31), 8750−8765.
(10) Pietsch, C.; Hoogenboom, R.; Schubert, U. S. *Angew. Chem., Int. Ed.* **2009**, *48* (31), 5653−5656.
(11) Qin, S.; Geng, Y.; Discher, D. E.; Yang, S. *Adv. Mater.* **2006**, *18* (21), 2905−2909.
(12) Li, Y.; Lokitz, B. S.; McCormick, C. L. *Angew. Chem., Int. Ed.* **2006**, *45* (35), 5792−5795.
(13) Hoogenboom, R.; Rogers, S.; Can, A.; Becer, C. R.; Guerrero-Sanchez, C.; Wouters, D.; Hoeppener, S.; Schubert, U. S. *Chem. Commun.* **2009**, *37*, 5582−5584.
(14) Discher, B. M.; Won, Y.-Y.; Ege, D. S.; Lee, J. C.-M.; Bates, F. S.; Discher, D. E.; Hammer, D. A. *Science* **1999**, *284* (5417), 1143−1146.
(15) Discher, D. E.; Eisenberg, A. *Science* **2002**, *297* (5583), 967−973.
(16) Antonietti, M.; Förster, S. *Adv. Mater.* **2003**, *15* (16), 1323−1333.
(17) Coelho, J.; Ferreira, P.; Alves, P.; Cordeiro, R.; Fonseca, A.; Góis, J.; Gil, M. *EPMA J.* **2010**, *1* (1), 164−209.
(18) Onaca, O.; Enea, R.; Hughes, D. W.; Meier, W. *Macromol. Biosci.* **2009**, *9* (2), 129−139.
(19) Han, S.; Hagiwara, M.; Ishizone, T. *Macromolecules* **2003**, *36* (22), 8312−8319.
(20) Lutz, J.-F.; Hoth, A. *Macromolecules* **2005**, *39* (2), 893−896.
(21) Lutz, J.-F. *J. Polym. Sci., Part A: Polym. Chem.* **2008**, *46* (11), 3459−3470.
(22) Moad, G.; Rizzardo, E.; Thang, S. H. *Aust. J. Chem.* **2009**, *62* (11), 1402−1472.
(23) Keddie, D. J.; Moad, G.; Rizzardo, E.; Thang, S. H. *Macromolecules* **2012**, *45* (13), 5321−5342.
(24) Pietsch, C.; Fijten, M. W. M.; Lambermont-Thijs, H. M. L.; Hoogenboom, R.; Schubert, U. S. *J. Polym. Sci., Part A: Polym. Chem.* **2009**, *47* (11), 2811−2820.
(25) Lutz, J.-F.; Akdemir, Ö.; Hoth, A. *J. Am. Chem. Soc.* **2006**, *128* (40), 13046−13047.
(26) Becer, C. R.; Hahn, S.; Fijten, M. W. M.; Thijs, H. M. L.; Hoogenboom, R.; Schubert, U. S. *J. Polym. Sci., Part A: Polym. Chem.* **2008**, *46* (21), 7138−7147.
(27) Ishizone, T.; Seki, A.; Hagiwara, M.; Han, S.; Yokoyama, H.; Oyane, A.; Deffieux, A.; Carlotti, S. *Macromolecules* **2008**, *41* (8), 2963−2967.
(28) Fournier, D.; Hoogenboom, R.; Thijs, H. M. L.; Paulus, R. M.; Schubert, U. S. *Macromolecules* **2007**, *40* (4), 915−920.
(29) Üzgün, S.; Akdemir, Ö.; Hasenpusch, G.; Maucksch, C.; Golas, M. M.; Sander, B.; Stark, H.; Imker, R.; Lutz, J.-F.; Rudolph, C. *Biomacromolecules* **2009**, *11* (1), 39−50.
(30) Cai, J.; Yue, Y.; Rui, D.; Zhang, Y.; Liu, S.; Wu, C. *Macromolecules* **2011**, *44* (7), 2050−2057.
(31) Hinton, T. M.; Guerrero-Sanchez, C.; Graham, J. E.; Le, T.; Muir, B. W.; Shi, S.; Tizard, M. L. V.; Gunatillake, P. A.; McLean, K. M.; Thang, S. H. *Biomaterials* **2012**, *33* (30), 7631−7642.
(32) Cho, S. H.; Jhon, M. S.; Yuk, S. H.; Lee, H. B. *J. Polym. Sci., Part B: Polym. Phys.* **1997**, *35* (4), 595−598.
(33) Bütün, V.; Armes, S. P.; Billingham, N. C. *Polymer* **2001**, *42* (14), 5993−6008.
(34) Liu, Q.; Yu, Z.; Ni, P. *Colloid Polym. Sci.* **2004**, *282* (4), 387−393.
(35) Plamper, F. A.; Ruppel, M.; Schmalz, A.; Borisov, O.; Ballauff, M.; Müller, A. H. E. *Macromolecules* **2007**, *40* (23), 8361−8366.
(36) Plamper, F. A.; Schmalz, A.; Müller, A. H. E. *J. Am. Chem. Soc.* **2007**, *129* (47), 14538−14539.
(37) París, R.; Quijada-Garrido, I. *Eur. Polym. J.* **2010**, *46* (11), 2156−2163.
(38) Yamamoto, S.-i.; Pietrasik, J.; Matyjaszewski, K. *Macromolecules* **2008**, *41* (19), 7013−7020.
(39) van de Wetering, P.; Zuidam, N. J.; van Steenbergen, M. J.; van der Houwen, O. A. G. J.; Underberg, W. J. M.; Hennink, W. E. *Macromolecules* **1998**, *31* (23), 8063−8068.
(40) Schilli, C. M.; Zhang, M.; Rizzardo, E.; Thang, S. H.; Chong, Y. K.; Edwards, K.; Karlsson, G.; Müller, A. H. E. *Macromolecules* **2004**, *37* (21), 7861−7866.
(41) Baines, F. L.; Billingham, N. C.; Armes, S. P. *Macromolecules* **1996**, *29* (10), 3416−3420.
(42) Kostiainen, M. A.; Pietsch, C.; Hoogenboom, R.; Nolte, R. J. M.; Cornelissen, J. J. L. M. *Adv. Funct. Mater.* **2011**, *21* (11), 2012−2019.
(43) Arotçaréna, M.; Heise, B.; Ishaya, S.; Laschewsky, A. *J. Am. Chem. Soc.* **2002**, *124* (14), 3787−3793.
(44) Kotsuchibashi, Y.; Ebara, M.; Yamamoto, K.; Aoyagi, T. *Polym. Chem.* **2011**, *2* (6), 1362−1367.
(45) Blanazs, A.; Armes, S. P.; Ryan, A. J. *Macromol. Rapid Commun.* **2009**, *30* (4−5), 267−277.
(46) Liu, S.; Armes, S. P. *J. Am. Chem. Soc.* **2001**, *123* (40), 9910−9911.
(47) Xu, J.; Luo, S.; Shi, W.; Liu, S. *Langmuir* **2005**, *22* (3), 989−997.
(48) Weiss, J.; Bottcher, C.; Laschewsky, A. *Soft Matter* **2011**, *7* (2), 483−492.
(49) Hua, F.; Jiang, X.; Zhao, B. *Macromolecules* **2006**, *39* (10), 3476−3479.
(50) Agut, W.; Brulet, A.; Schatz, C.; Taton, D.; Lecommandoux, S. *Langmuir* **2010**, *26* (13), 10546−10554.
(51) Farnham, W. B., PCT Int. Appl. WO 2005113493, A1 20051201, 2005.
(52) Keddie, D. J.; Guerrero-Sanchez, C.; Moad, G.; Rizzardo, E.; Thang, S. H. *Macromolecules* **2011**, *44* (17), 6738−6745.
(53) Guerrero-Sanchez, C.; Keddie, D. J.; Saubern, S.; Chiefari, J. *ACS Comb. Sci.* **2012**, *14* (7), 389−394.
(54) Keddie, D. J.; Guerrero-Sanchez, C.; Moad, G.; Mulder, R. J.; Rizzardo, E.; Thang, S. H. *Macromolecules* **2012**, *45* (10), 4205−4215.
(55) Koppel, D. E. *J. Chem. Phys.* **1972**, *57* (11), 4814−4820.

(56) Ohshima, H. *J. Colloid Interface Sci.* **1994**, *168* (1), 269−271.
(57) Moad, G.; Chong, Y. K.; Postma, A.; Rizzardo, E.; Thang, S. H. *Polymer* **2005**, *46* (19), 8458−8468.
(58) Sahnoun, M.; Charreyre, M.-T.; Veron, L.; Delair, T.; D'Agosto, F. *J. Polym. Sci., Part A: Polym. Chem.* **2005**, *43* (16), 3551−3565.
(59) Guillaneuf, Y.; Castignolles, P. *J. Polym. Sci., Part A: Polym. Chem.* **2008**, *46* (3), 897−911.
(60) Israelachvili, J. N., *Intermolecular and Surface Forces*. 3rd ed.; Elsevier, Academic Press: Amsterdam, 2011.
(61) Zhang, L.; Eisenberg, A. *J. Am. Chem. Soc.* **1996**, *118* (13), 3168−3181.
(62) Holder, S. J.; Sommerdijk, N. A. J. M.; Williams, S. J.; Nolte, R. J. M.; Hiorns, R. C.; Jones, R. G. *Chem. Commun.* **1998**, *14*, 1445−1446.